CHAPTER 5

X-RAY DIFFRACTION AND DIELECTRIC SPECTROSCOPY STUDIES ON A PARTIALLY FLUORINATED FERROELECTRIC LIQUID CRYSTAL COMPOUND FROM THE FAMILY OF TERPHENYL ESTERS

Part of the work was presented at the XVIII conference on Liquid Crystals at Augustow, Poland, September 2009 and was published in Liquid Crystals, Vol. 39, No. 10, 1196–1203' October 2012

5.1. INTRODUCTION

Ferroelectric liquid crystals are only known intrinsic polar fluid materials that possess the ferroelectric, electrooptic, piezoelectric and pyroelectric properties of solid polar dielectric materials with the physical flow characteristics of liquids. Moreover, some such compounds show antiferroelectric SmC_A^*, ferroelectric SmC^* and paraelectric SmA^* phases making them attractive from both theoretical and application points of view. Liquid crystals with SmC_A^* and SmC^* phases attracted many researchers because these materials are suitable for applications in various display devices [315-318]. Because liquid crystals with fluorosubstituents show low viscosity, low conductivity, and high chemical and thermal stability, many liquid crystals with fluorosubstituents both in the cores and alkoxy chains were designed and synthesized in both non-chiral and chiral systems [70,319-323].

In this chapter we present the results of investigation on the partially fluorinated chiral compound, (S)-4″-(6-perfluoropentanoyloxyhexyl-1-oxy)-2′,-3′-difluoro - 4 - (1-methylheptyl oxycarbonyl) -[1,1′:4′,1″]- terphenyl [acronym 5F6T(2′,3′F)], which exhibits antiferroelectric, ferroelectric and paraelectric phases. The compound was synthesized by P. Kula et al [324]. In the ferroelectric SmC^* phase, chiral molecules are spontaneously tilted at an angle with respect to the layer normal. Due to chirality and polarity of the molecules, a macroscopic spontaneous polarization is observed in a direction normal to the tilt plane. The direction of the tilt and the spontaneous polarization slowly precess as one moves along the layer normal. As a result, a helical structure is formed, with a helical period of the order of the wavelength of visible light. In the antiferroelectric SmC_A^* phase, the molecules are also tilted but the direction of the tilt alternates when one moves from one smectic layer to the other. From frequency dependent dielectric study in the SmC_A^*, SmC^* and SmA^* phases one can get idea about their collective mode relaxation behaviour.

It was discussed in chapter 2 that two important relaxation modes, viz. Goldstone mode (GM) and soft mode (SM), are observed in FLC materials. The Goldstone mode shows up throughout the SmC^* phase because of the phase fluctuations in the azimuthal orientation of the directors whereas the soft mode appears practically in the neighbourhood of the SmC^* - SmA^* transition point because of the fluctuation in the tilt angles of the molecular directors. As the Goldstone mode dielectric increment is usually large compared to the soft mode increment it is difficult to study the soft mode properties in the SmC^* phase. Yet, this problem can be overcome by applying a DC electric field to the SmC^* phase, so-called the bias field, being strong enough to unwind the helical arrangement of the polarization vector. In such

situation the Goldstone mode is suppressed and the soft mode can be studied almost separately. In AFLC materials usually double relaxation processes with critical frequencies in kilohertz and megahertz range are observed. Low frequency mode (P_L), known as inphase antiferroelectric mode, is result of collective reorientation of the molecules in the same direction and the high frequency mode (P_H), known as antiphase antiferroelectric mode, arises due to reorientation in the opposite direction [325,326].

Along with frequency dependent dielectric study spontaneous polarization (P_S), which is a measure of order parameter and on which the switching time of the FLC display devices depends, has also been measured. In addition, from small angle X-ray diffraction study nature of temperature dependence of layer thickness and tilt angle in different phases have been determined.

5.2. EXPERIMENTAL PROCEDURE

The Phase behaviour of the compound 5F6T(2',3'F) has been investigated by polarizing microscope equipped with the heating stage. The heating/cooling rate was 1.0 ^{0}C / min and the measurement accuracy was ± 0.1^{0}C. Setaram 141 calorimeter was used for DSC study. X-ray diffraction photographs were taken using a home-built high temperature camera, orienting the sample by magnetic field [106,297]. The diffraction photographs, scanned by a HP2200C scanner in 24 bit RGB colour format, were analyzed to find the smectic layer spacings (d) using Bragg equation, $d = n\lambda/2\sin\varphi$. Tilt angles ($\theta_t$) have been calculated using the relation $\theta_t = \cos^{-1}(d/d_A)$, where d_A is the layer spacing at lowest temperature in SmA* phase [327].

Dielectric and electro-optical studies were performed using ITO coated homogeneous cells (with sheet resistance of about 20 Ω/□).). Aligning layers (nylon 6, 100-120 nm) were spin coated on the ITO layers at 3000 rpm and baked at 180 ^{0}C for one hour and then rubbed uni-directionally. Cells of three different thicknesses (3.2 μm, 5.2 μm and 8.1 μm) were used. Complex dielectric permittivity measurements were made using HP 4192A and Hioki 3532-50 impedance analyzers, temperature was controlled within ± 0.1^{0}C using Eurotherm controller (2216e). Automatic data acquisition arrangement was made using RS232 interface with a PC. Reversal current method [168] was used to measure spontaneous polarization (P_S), following procedure described elsewhere [328]. An oscilloscope (HP 500 MHz Infinium) was used to record the polarization peak. Details of experimental procedure have already been discussed in chapter 2.

5.3. RESULTS AND DISCUSSION

5.3.1. OPM, DSC AND X-RAY STUDY

The molecular structure of the investigated compound 5F6T (2' 3' F) and phase transition temperatures (in ^{0}C) obtained from OPM study are presented in **Figure 5.3.1.** The molecule has chirality only at one end, it is partially fluorinated in the other end, also in the central phenyl ring. It was found to exhibit antiferroelectric phase (SmC_A^*) over a relatively low temperature range (9.1^{0}C) but ferroelectric SmC^* phase and paraelectric SmA^* phase over a wide temperature range, 21.3^{0}C and 20.4^{0}C respectively.

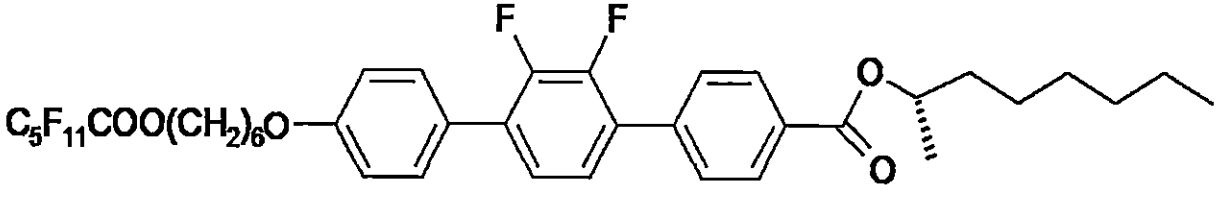

Cr 41.1 SmC_A^* 50.2 SmC^* 71.5 SmA^* 91.9 Iso

Figure 5.3.1. *Molecular structure and transition temperatures of 5F6T (2' 3' F)*

Melting enthalpy of investigated compound is typical for these homologous series and is equal to 24.4 kJ/mol, transition from antiferroelectric to ferroelectric phase could not be observed on DSC thermogram, similar situation was observed for seventh homologue [7F6T (2'3'F)], for other homologues enthalpy of SmC_A* to SmC* phase transition was on the level of 30 J/mol and was clearly visible on DSC curve. For ferroelectric to paraelectric SmA^* phase and SmA* to Isotropic phase transitions enthalpy was typical and equal 300 J/mol and 4.2 kJ/mol respectively.

Photomicrographs of the observed textures in cooling sequence are shown in **Figure 5.3.2.** Typical fan shaped texture is observed in SmA^* phase which is superimposed by an equidistant line pattern due to the helical superstructure at SmA^*- SmC* transition. In SmC* phase domains with equidistant line pattern is clearly visible which transforms into broken fan shape texture with helical pattern in SmC_A* phase as described by Dierking [102]. Observed phases were also confirmed by miscibility study.

SmA^* at 84 ^0C

SmA^* to SmC^* transition at 72 ^0C

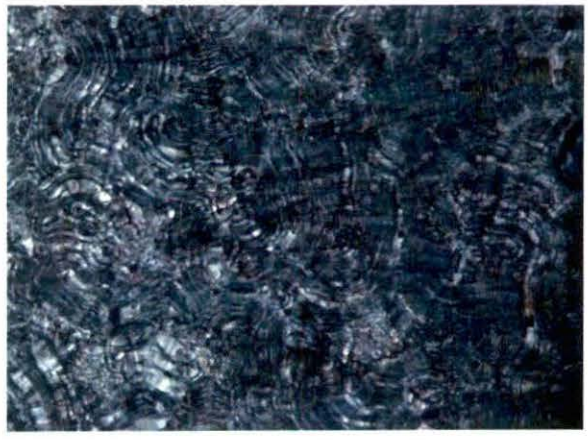

SmC^* at 55 ^0C

SmC^* to SmC_A^* transition at 50 ^0C

SmC_A^* at 43 ^0C

Figure 5.3.2. *Observed textures of chiral smectic phases during cooling.*

Effect of fluorination in the core structure of the molecule can be seen from **Table 5.3.1**. When a fluorine atom is introduced in 2- position of the carbonyloxy group {5F6T→5F6T(2F)} substantial drop in the melting point(23.9^0) is observed. A further drop of 19.4^0 is observed on the introduction of additional fluorine atom {5F6T(2F)→5F6T(2,3F)}.

Table 5.3.1

Sample (Acronym)	Molecular structure and transition temperatures
5F6T	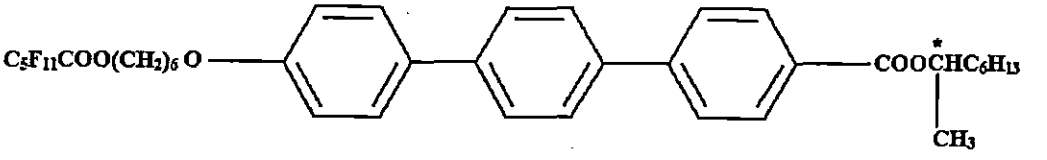 Cr 118.2°C SmC_A^* 138°C SmA* 155.7°C I [324]
5F6T(2F)	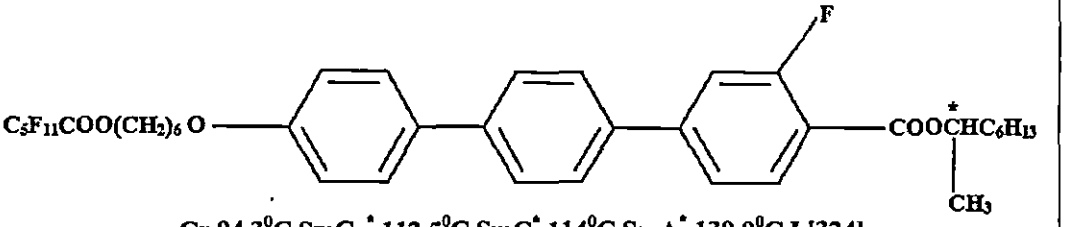 Cr 94.3°C SmC_A^* 112.5°C SmC* 114°C SmA* 139.9°C I [324]
5F6T(2,3F)	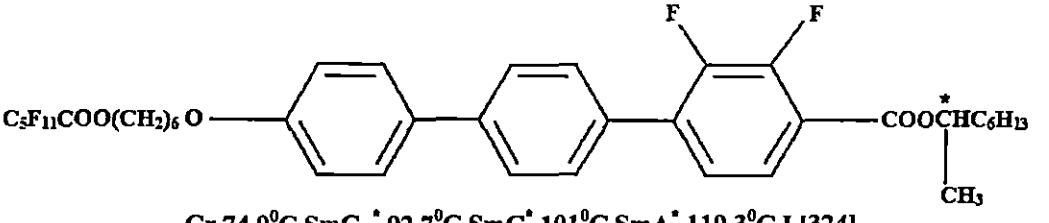 Cr 74.9°C SmC_A^* 92.7°C SmC* 101°C SmA* 119.3°C I [324]
5F6T(2',3'F	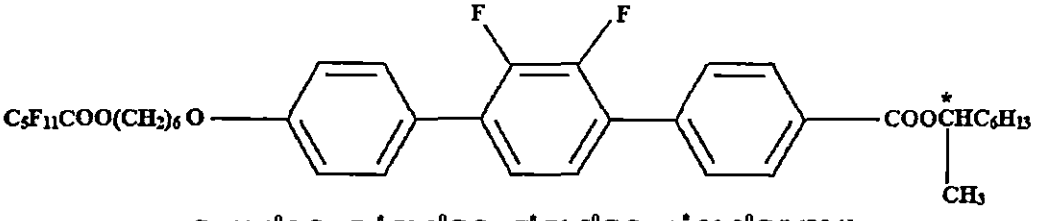 Cr 41.1°C SmC_A^* 50.2°C SmC* 71.5°C SmA* 91.9°C I [324]
4F3R	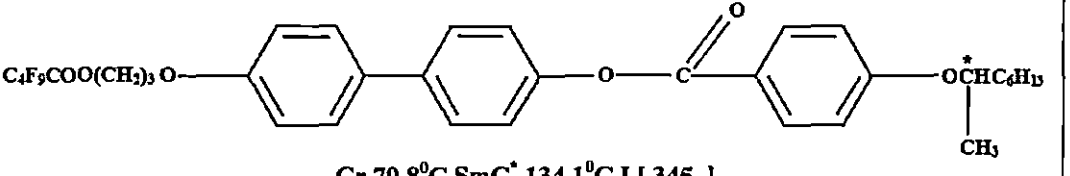 Cr 79.8°C SmC* 134.1°C I [345]
TP1	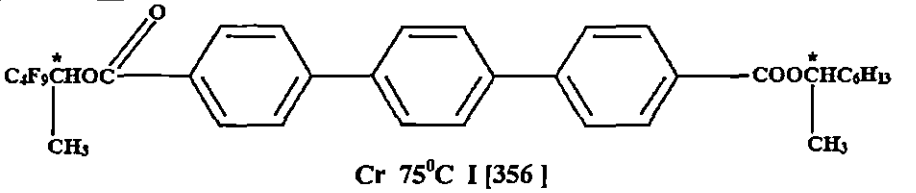 Cr 75°C I [356]

But when the two fluorine atoms are introduced in the central phenyl ring {5F6T(2,3F)→5F6T(2′,3′F)} observed drop in melting point is 33.8^0. In other words drastic drop in melting point as large as 77.1^0, occurs on the lateral substitution of two fluorine atoms in the central phenyl ring compared to unsubstituted molecule {5F6T→5F6T(2′,3′F)}. However, in the above sequential fluorination stability of SmC^* phase increases from 0^0 {no SmC^* phase in 5F6T} to 21.3^0 {5F6T(2′,3′F)} at the cost of the stability of SmC_A^* phase 19.8^0 in 5F6T and 9.1^0 in 5F6T(2′,3′F). Thus lateral fluorination in the core structure has pronounced effect on the phase behavior and stability.

Effect of rigidity of the core structure on the phase behavior can be seen by considering the example of 4F3R molecule (**Table 5.3.1**). Here the biphenyl ring is connected to the third phenyl ring by the —COO group, however the end chains are more or less similar. Melting point is high, comparable to that of 5F6T(2,3F) ; only ferroelectric phase is observed over a considerable temperature range(54.8^0) ; it goes directly to isotropic phase without exhibiting antiferroelectric phase at temperatures below and paraelectric phase at above the ferroelectric phase. It is interesting to note further that a terphenyl compound TP1 (**Table 5.3.1**) having chiral centers at both ends is not mesogenic at all.

The X-ray diffraction photographs observed in different phases are shown in **Figure 5.3.3** at three representative temperatures. Temperature variation of smectic layer spacing (d) is shown in **Figure 5.3.4**. In SmA^* phase layer spacing remains nearly constant. It shows a step jump at SmA^* - SmC^* transition and about 3.3% layer shrinkage is observed. However, no such shrinkage is exhibited at SmC^* - SmC_A^* transition. Within both the SmC^* and SmC_A^* phases layer thickness decreases with decreasing temperature. As a result, with increasing temperature tilt angle in SmC_A^* phase decreases from 22.2^o to 19.5^o, in SmC^* phase it also

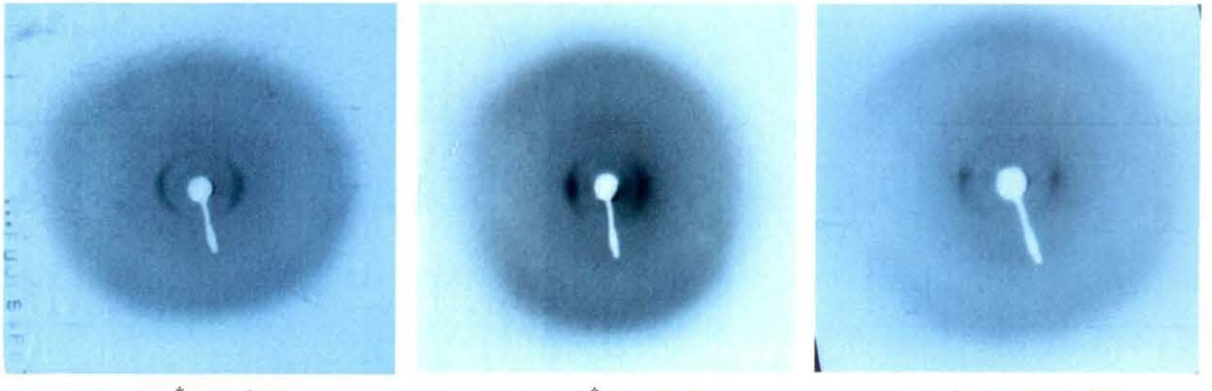

SmC_A^* (48 °C) **SmC^* (66 °C)** **SmA* (79 °C)**

Figure 5.3.3. *X-ray diffraction photographs in different chiral smectic phases.*

decreases but near SmC^* - SmA^* transition the rate of decrement is quite high as shown in **Figure 5.3.5**. Thus from the point of view of layer shrinkage the material behaves like a regular ferroelectric, not de Vries type where virtually no layer shrinkage is observed at SmA^* to SmC^* transition [329,330].

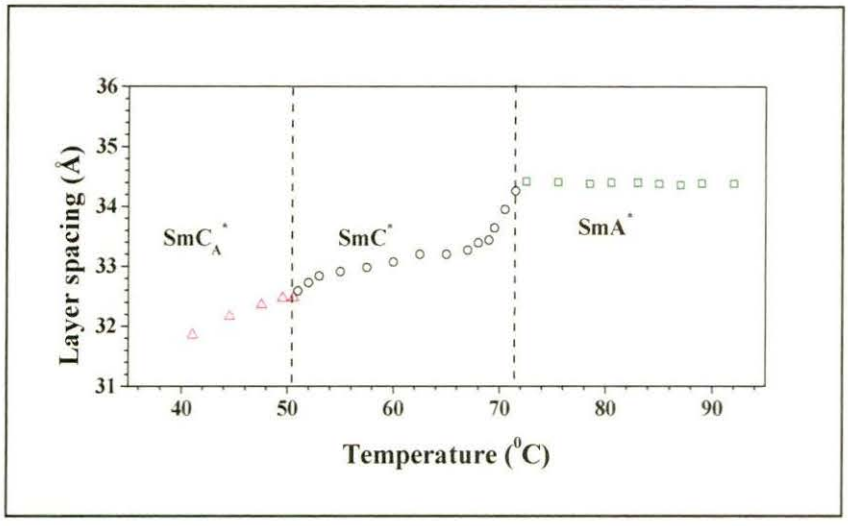

Figure 5.3.4. *Temperature variation of layer spacings in different chiral smectic phases.*

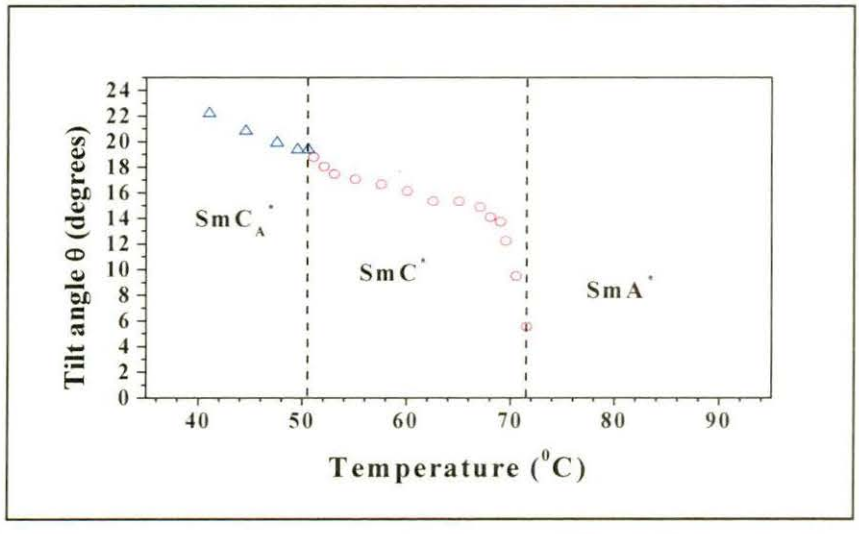

Figure 5.3.5. *Temperature variations of tilt angles in different chiral smectic phases.*

Nonlinear increase of d with temperature had also been reported in both ferroelectric SmC^* and antiferroelectric SmC^*_A phases from X-ray diffraction using synchrotron radiation [330]. Continuous layer expansion on lowering of temperature or almost temperature independent layer spacing (hence free from chevron defects) has also been observed in pure or FLC mixtures [331].

To elucidate the structure of the molecule 5F6T(2',3'F), its geometry was optimized using PM3 molecular mechanics method in *Hyperchem* software package [241]. The optimized structure of the molecule, direction of principal axes along with the direction of its electric dipole moment is shown in **Figure 5.3.6.** Optimized length of the molecule is 39.5Å. It shows comparatively lower dipole moment (1.80 D), with components –1.50, –0.56, 0.81 D along the three principal moments of inertia axes. Corresponding moments of inertia are found to be 51.6 x10^{-46}, 18895.0 x10^{-46} and 19173.0 x10^{-46} kgm^2.

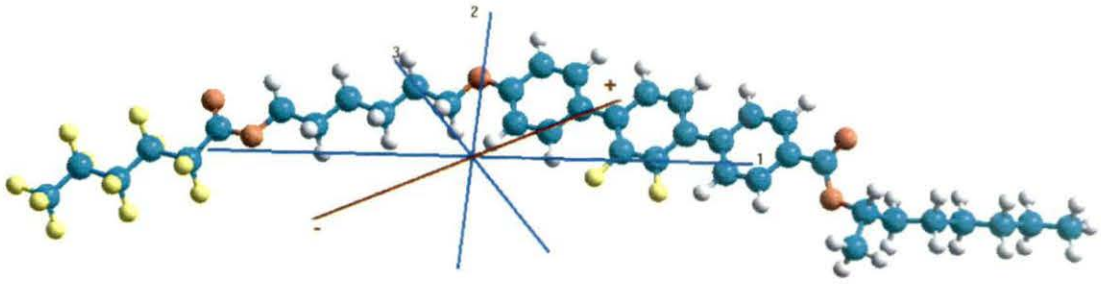

Figure 5.3.6. *5F6T(2',3'F) molecule in optimized geometry along with of orientation of dipole moment with respect to principal inertial axes.*

5.3.2. FREQUENCY AND TEMPERATURE DEPENDENT DIELECTRIC STUDY

Response of the material in an ac field was studied first in a dielectric cell of thickness 5.2 μm. Temperature variation of real and imaginary parts of dielectric constant (ε' and ε") at some selected temperatures are shown in **Figure 5.3.7** which shows clear discontinuities at the transition points.

In the observed frequency range and in planar orientation geometry, only collective mode relaxation behavior could be studied. However, only GM relaxation is observed in both ferro- and antiferroelectric phases. SM is not observed in SmC* without bias field. When a dc bias field of 5V was applied, SM is observed near SmC*- SmA* transition in the temperature range 71-75 ^{0}C. No SM or antiphase azimuthal angle fluctuation mode (which is described as ***process 1*** in reference [332]) is observed in SmC_A*, probable reason for this will be described later.

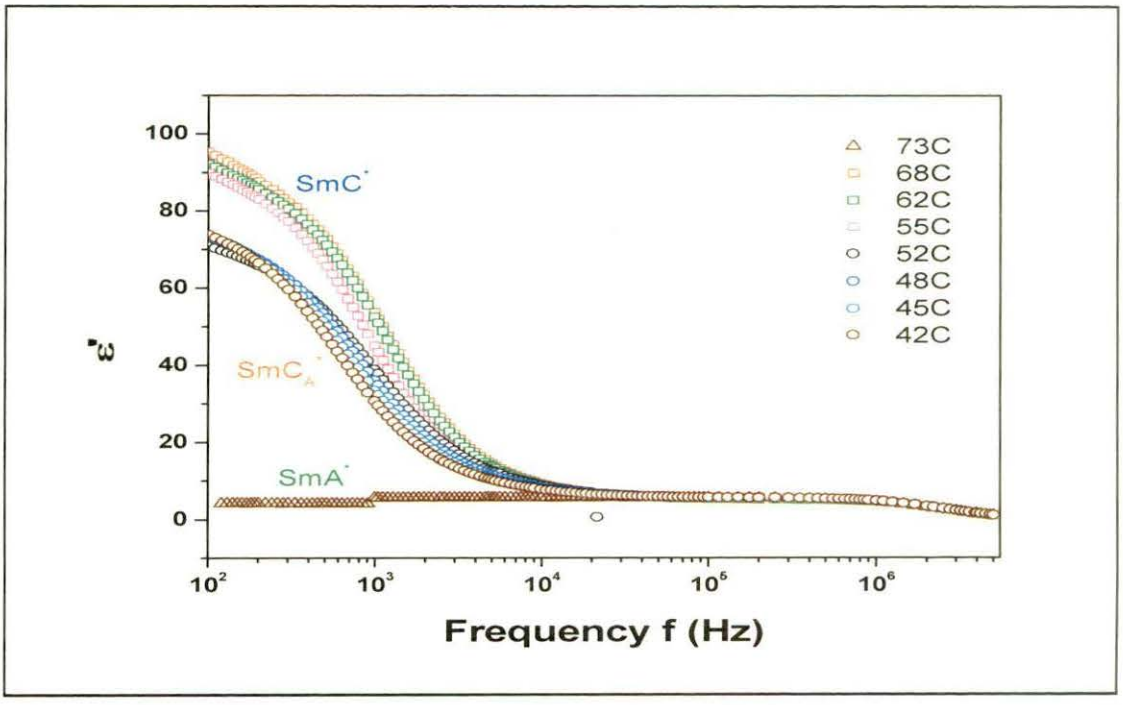

(a)

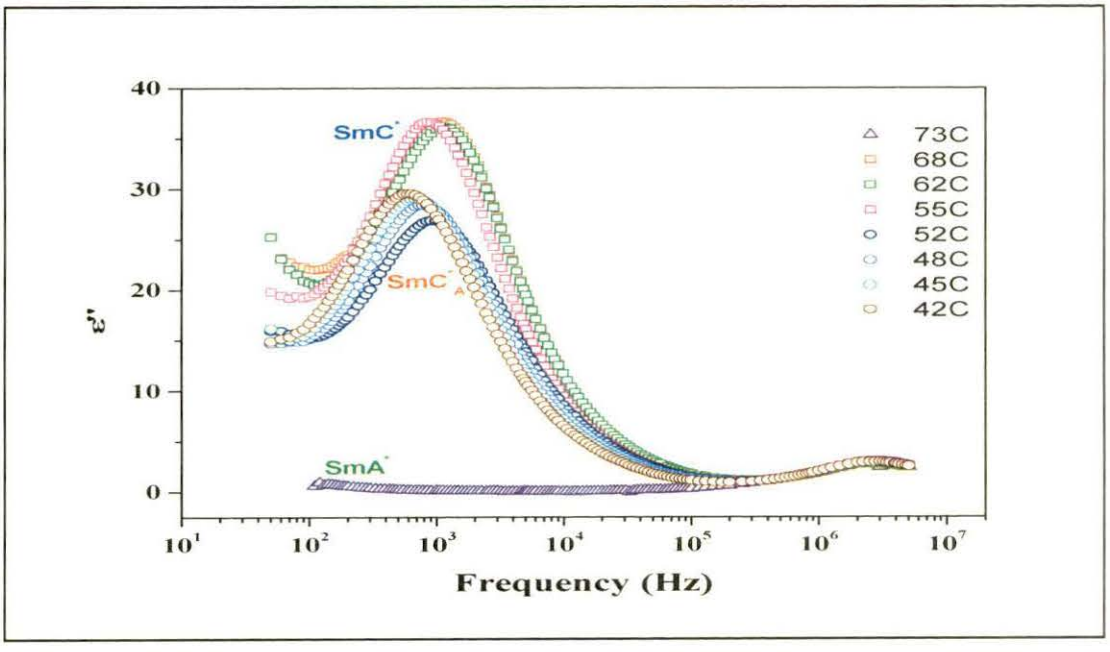

(b)

***Figure 5.3.7(a)**. Real part(ε') and (**b**)Imaginary part (ε'') of dielectric constants with frequency at different temperatures*

It is seen that GM critical frequency (f_C) increases very slowly and SM critical frequency increases very fast with temperature, shown in **Figure 5.3.8(a)**. This is expected according to the generalized Landau model of T. Carlsson *et al* [162]. In the literature both temperature independent f_C [333-337] and increase of f_C with temperature [338,339] are reported in pure and FLC mixtures.

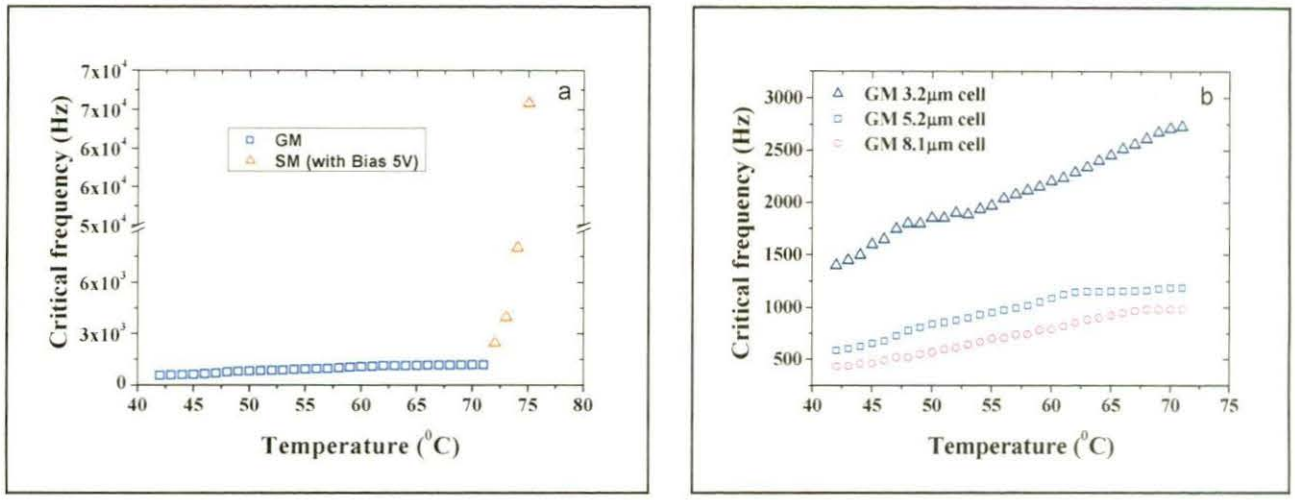

Figure 5.3.8(a). *Temperature variation of GM and SM relaxation frequency (5.2 μm cell) and* ***(b)*** *thickness dependence of GM relaxation frequency.*

Since surface anchoring will have influence on the relaxation behaviour of the molecules in the planar orientation, especially in thin cells GM critical frequencies are expected to depend on the cell thickness. To explore this we performed the relaxation experiment in two more cells with identical surface treatment but one with smaller thickness (3.2 μm) and other with larger thickness (8.1 μm). It is seen that the critical frequency decreases with the increase of thickness as shown in **Figure 5.3.8(b),** rate of decrement also follows same trend. For examples observed values are 1400Hz, 590Hz and 430Hz at 42°C in SmC_A* phase and 2675Hz, 1182Hz and 980Hz at 69°C in SmC* phase in cells of thicknesses 3.2 μm, 5.2 μm and 8.1 μm respectively. Increase in GM relaxation frequency with decreasing cell thickness indicates that the molecular motion is restricted in thin cells due to strong surface interactions. Similar behaviour was observed in room temperature FLC mixtures [340,341].

Dielectric spectra was fitted to the Cole–Cole function [342,343] as detailed in chapter 2, to remove the low frequency conductivity effect and high frequency ITO effect and also to take into account the distribution parameters(α).

As a representative example, fitted absorption spectra in SmC* phase at 62^{0}C in cell of thickness 5.2 μm is shown in **Figures 5.3.9.** Values of fitted parameters along with GM, ITO and σ curves are also shown in the figure. Since real and imaginary parts of dielectric constants are related through Kramers-Kronig relation, Cole-Cole plot of the same data is also shown in **Figure 9.3.10** to see how good is the fitting for ε' and ε''. Observed values of

distribution parameter (α) (0.13-0.19) signify that the GM relaxation process is not strictly Debye type, however, nature of ITO peak, was definitely Debye type.

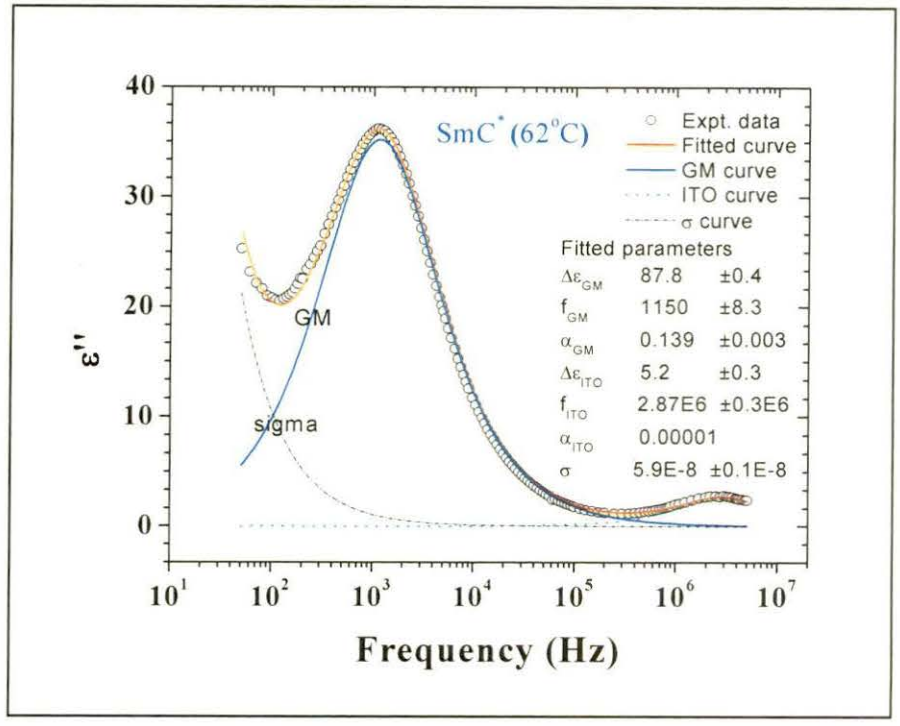

Figure 5.3.9. *Fitted spectra in SmC* phase (62°C), cell thickness 5.2 μm along with observed data. GM, ITO and σ curve are also shown separately along with fitted parameters.*

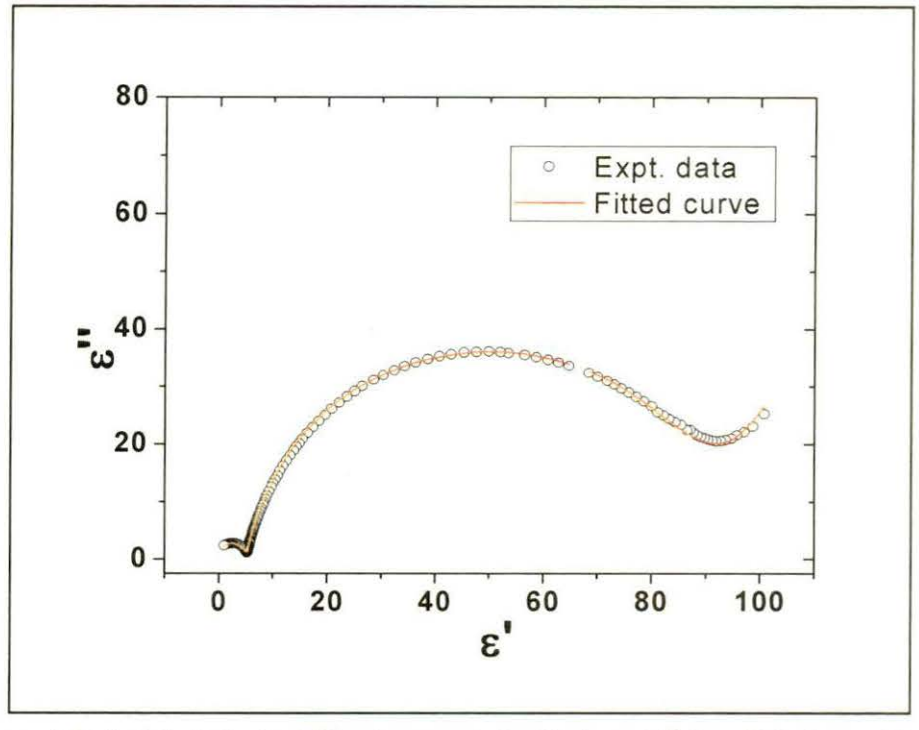

Figure 9.3.10. *Cole-Cole plot of fitted spectra in SmC* phase (62°C), cell thickness 5.2 μm.*

It is further observed that the dielectric increment ($\Delta\varepsilon$) changes discontinuously at transitions (**Figure 5.3.11**). Although there is sharp decrease in $\Delta\varepsilon$ at SmC_A^* - SmC^* transition, magnitude of $\Delta\varepsilon$ in SmC_A^* phase is very large (~72) which is usually of the order of one or at the most two as reported in literature for typical SmC_A^* [161,332,344] or for its variant like $SmC_A^*(1/3)$ and $SmC_A^*(1/2)$ [334]. Repetition of relaxation experiments with different cells confirmed above observation. It is not possible to give any definitive explanation for this, however, it may be thought that due to surface interactions under the confined geometry of thin dielectric cell (5.2 μm) the material is probably showing ferrielectric type behavior although in bulk it shows antiferroelectric phase. Absence of DSC signal and relaxation behavior related to anti-phase azimuthal angle fluctuation as well as continuous change in layer thickness and spontaneous polarization at SmC^*- SmC_A^* transition (described below) support this view. It may be mentioned here that Panarin *et al* [161] observed that in thin cells some ferrielectric subphases are suppressed by the surface interactions.

Dielectric increment ($\Delta\varepsilon$) within the ferroelectric phase is found to increase considerably with temperature, rate of increment is faster as SmC^*- SmA^* transition is approached. Such increase has been reported in several FLC compounds [334,335]. Increase of dielectric strength with temperature may be explained if one assumes stronger biquadratic coupling between tilt and polarization compared to bilinear one in the expression for free energy density in generalized Landau model [162]. But $\Delta\varepsilon$ should decrease near T_C in such situation which is not observed in the present study.

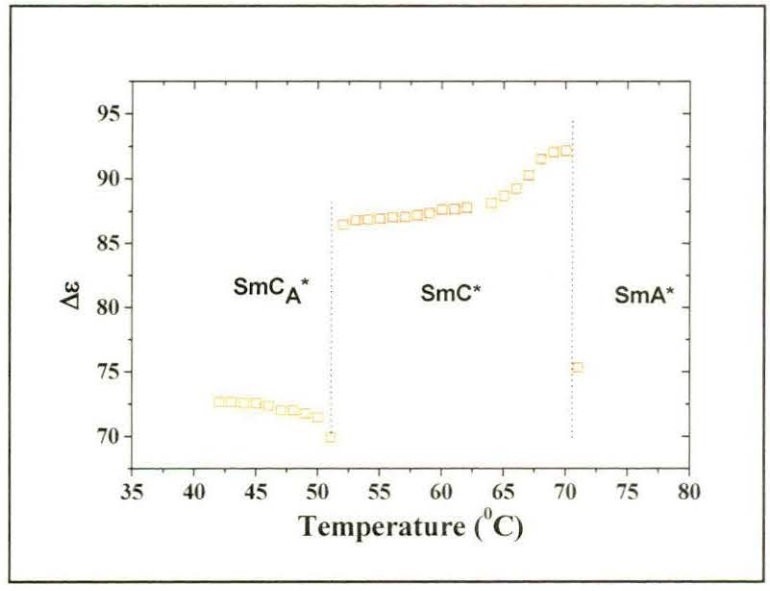

Figure 5.3.11. *Temperature variation dielectric increment ($\Delta\varepsilon$) (cell thickness 5.2 μm).*

Spontaneous polarization (P_S), the secondary order parameter of an FLC compound, was measured as a function of temperature. Input triangular pulse and output signal across the liquid crystal cell captured in a digital oscilloscope are shown in **Figure 5.3.12.** As depicted in **Figure 5.3.13,** spontaneous polarization decreases slowly with temperature, are found to vary between 74.1 -118.7 nC/cm^2. Thus observed P_S is quite high. No discontinuity at SmC_A* - SmC* transition is observed. Similar behaviour was reported in other AFLCs [323].

For comparison it may be pointed out that the compound 4F3R shows P_S about 41.7 nC/cm^2 near Cr-SmC* transition [345]. Compounds with similar backbone as that of 4F3R, only with different fluorinated carboxylate chain (Viz. C_4F_9COO-$(CH_2)_6$ and $C_5F_{11}COO$-$(CH_2)_6$) exhibit P_S of about 50 nC/cm^2 near Cr-SmC* transition but when longer fluorinated chain $C_8F_{17}COO$-$(CH_2)_2$ is introduced P_S increases to about 93 nC/cm^2 [346]. On the introduction of another carboxylate group in between the phenyl group and the chiral centre in the above compounds P_S drastically increases to above 200 nC/cm^2 [328,347]. Present investigated compound ($C_5F_{11}COO(CH_2)_6$-O-Ph-Ph(2′, 3′ F)-Ph-COO-$CH(CH_3)$-C_6H_{13}) showed P_S value 118.7 nC/cm^2. Thus both core structure and chain length have pronounced effect on the magnitude of spontaneous polarization.

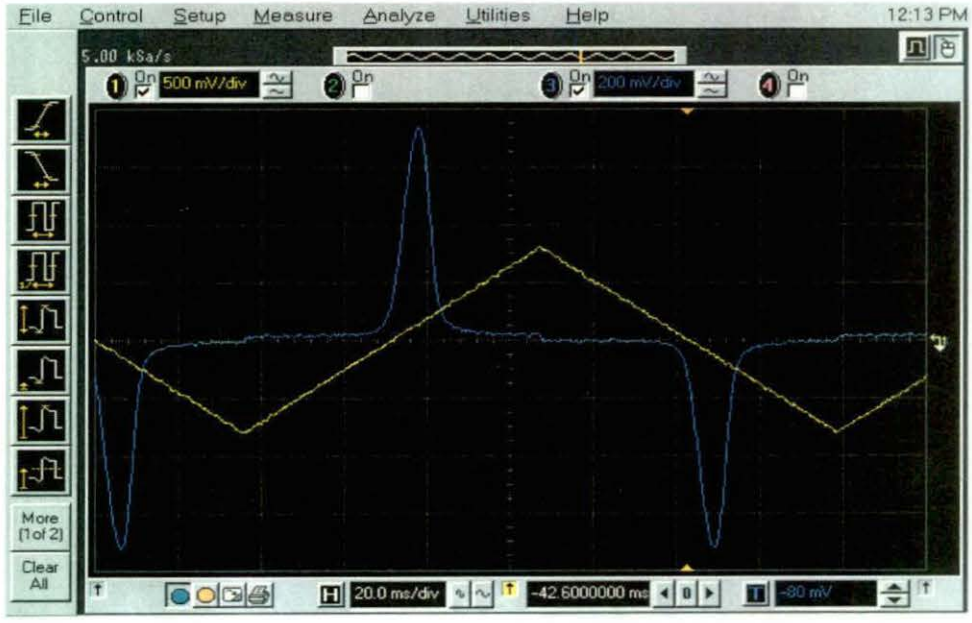

Figure 5.3.12. *Input and output signals captured in a digital oscilloscope at 44°C*

It was noted in chapter 2 that switching time (τ) of a SSFLC device is given by [70]

$$\tau = \frac{\gamma \sin\theta}{P_S E}$$

For portable devices of low power consumption the applied voltage E needs to be low, hence low tilt(θ), low viscosity(γ) and high P_S are required for switching time to be low. But a high value of P_S causes a current flow through the cell, which is undesirable. So a low viscosity is desirable and a moderate level of Ps is required for a short switching time.

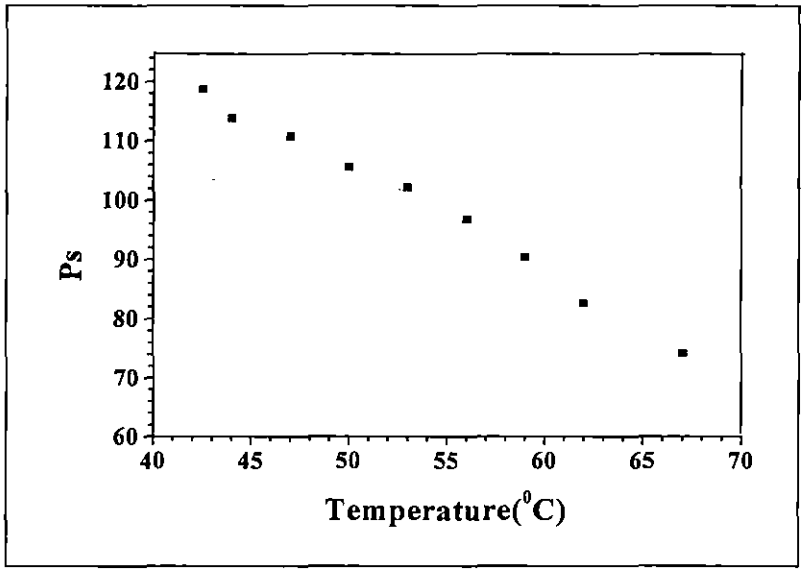

Figure 5.3.13. *Variation of spontaneous polarization (P_S) with temperature. Line through the experimental points is guide to the eye only*

Rotational viscosity (γ) in SmC^* phase was determined using the following relation derived from generalized Landau model [162]

$$\gamma = \frac{1}{4\pi\varepsilon_o}\frac{1}{\Delta\varepsilon_g f_g}\left(\frac{P_S}{\theta}\right)^2$$

$\Delta\varepsilon_g$, Goldstone mode dielectric strength, f_g, Goldstone mode relaxation frequency were determined from dielectric study and tilt angle (θ) was obtained from X-ray measurements. Similar expression was used to find its value in SmC_A^* phase. Variation of γ with temperature is shown in **Figure 5.3.14.** It is observed that viscosity decreases quite fast with temperature in a non-linear manner, rate of decrement is different in antiferroelectric and ferroelectric phases. Applying Arrhenius law to the above rotational viscosity data, the activation energy can be calculated using the relation, $\gamma \propto e^{E_a/k_BT}$, where E_a is the activation energy for the molecular rotation on the cone when the AC electric field is applied to the FLC material, k_B is the Boltzmann constant. Activation energy in SmC^* was found to be 48.14 kJ/mole, from linear least squares fit of the plot of lnγ vs 1000/T curve shown in **Figure 5.3.15** which is almost half of the value (97.09 kJ/mole) found in 4F3R[345] . Optimizing the geometry of the

5F6T(2',3'F) using Hyperchem it is found that its dipole moment is only 1.80 D, considerably less than the dipole moment of 4F3R (4.25D). Stronger dipole-dipole interaction between molecules of 4F3R may be responsible for higher activation energy.

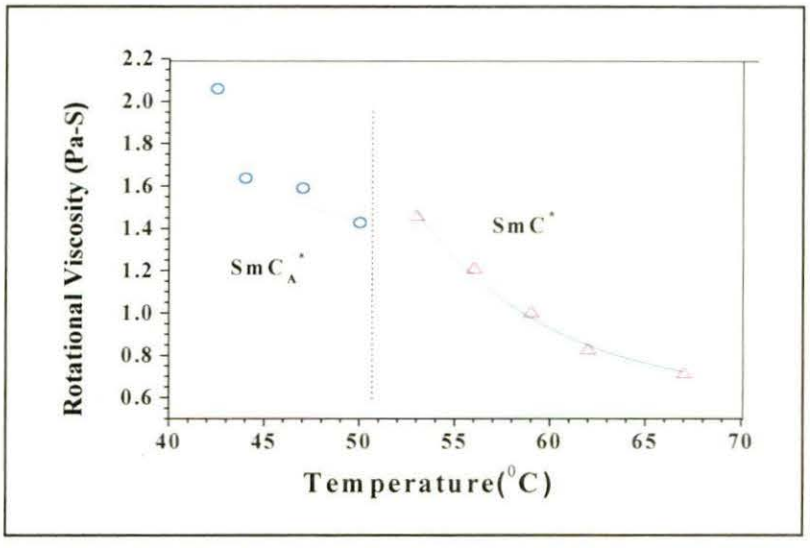

Figure 5.3.14. *Temperature variation of rotational viscosity of 5F6T(2',3'F).*

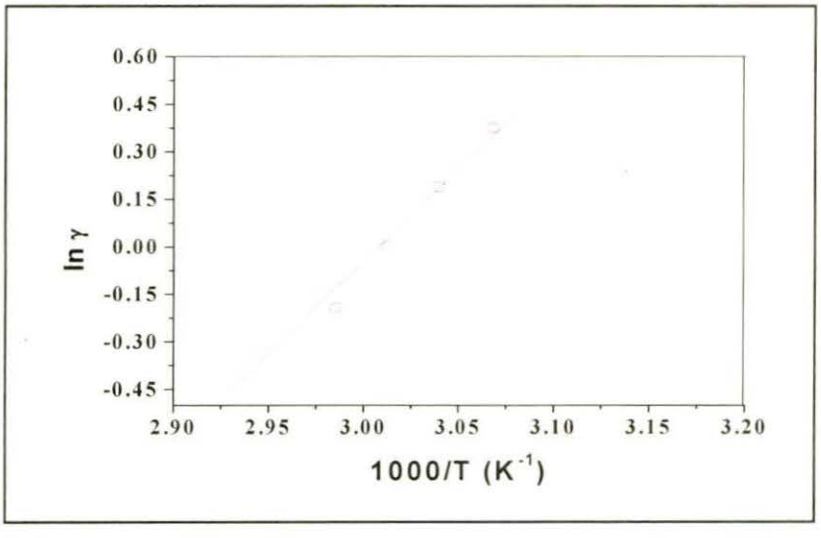

Figure 5.3.15. *Variation of lnγ against 1000/T in SmC* phase.*

5.4. CONCLUSIONS

Partially fluorinated compound, 5F6T(2',3'F)], which exhibits antiferroelectric SmC_A^*, ferroelectric SmC^* and paraelectric SmA^* phases, has been investigated by OPM, DSC, X-ray diffraction and frequency dependent dielectric spectroscopy methods. Typical fan shaped

texture in SmA^* phase, domains with equidistant line patterns due to helicoidal structure in SmC^* phase and broken fan texture with sign of helical pattern in SmC_A^* phase are observed. Rigidity of the core structure and its lateral fluorination are found to have pronounced effect on the phase behavior and on the stability of the antiferroelectric and ferroelectric phases. X-ray studies reveal that the layer thickness remains almost constant in SmA* phase but within SmC^* and SmC_A^* phases it decreases with decreasing temperature, a step jump is observed only at SmA^* - SmC^* transition which corresponds to about 3.3% layer shrinkage. As a result, tilt angle in SmC_A^* phase decreases slowly with increasing temperature, varies from 22.2° to 19.5°, in SmC^* phase it decreases from 18.8° to 5.5°, the rate of decrement is very sharp near SmC^* - SmA^* transition. From the point of view of layer shrinkage at SmA^*- SmC^* transition the compound behaves like regular ferroelectric, not de-Vries type. Molecular mechanics calculation reveals that the molecules possess a dipole moment of 1.80 D. Spontaneous polarization, determined by reversal current method, is observed to be quite high and varies between 74.1 - 118.7 nC/cm^2. Real and imaginary parts of dielectric constants, ε' and ε'' show discontinuous change at transition temperatures. Only Goldstone Mode (GM) relaxation is observed in both ferroelectric and antiferroelectric phases. Fitted data shows that the GM peak is Cole-Cole type. Soft Mode (SM) is not observed in SmC* without bias field, but on application of bias field SM is observed near SmC*- SmA* transition. Temperature dependence of GM and SM is found to be consistent with the predictions of generalized Landau model. No SM or antiphase azimuthal angle fluctuation mode is observed in SmC_A*.

Due to surface interactions under the confined geometry of thin dielectric cell (5.2 μm) the material is probably showing ferrielectric type behavior although in bulk it shows antiferroelectric phase, hence no SM or anti-phase antiferroelectric mode is observed. High value of ε' in SmC_A* absence of DSC signal and relaxation behavior related to antiphase azimuthal angle fluctuation as well as continuous change in layer thickness and spontaneous polarization at SmC*- SmC_A* transition support this view.

GM relaxation frequency is found to decrease with increasing cell thickness which indicates that the molecular motion is restricted in thin cells due to strong surface interactions. Rotational viscosity, calculated utilizing dielectric and X-ray data, is found to decrease quite fast in a non-linear manner, rate of decrement is different in ferro and antiferroelectric phases. In SmC^* phase activation energy for the process is found to be 48.14 kJ/mole.